Practical aspects of 13C surface receive coils with active decoupling and tuning circuit

Nilsson, Daniel ; Mohr, Johan Jacob; Zhurbenko, Vitaliy

Published in:
Proceedings of European Microwave Conference 2012

Publication date:
2012

Practical Aspects of 13C Surface Receive Coils with Active Decoupling and Tuning Circuit

Daniel T. P. Nilsson[1], Johan J. Mohr[2], and Vitaliy Zhurbenko[3]

Technical University of Denmark, Department of Electrical Engineering
Ørsteds Plads, Building 348, DK-2800 Kgs. Lyngby, Denmark
[1]danielnilsson@alumni.dtu.dk, [2]jm@elektro.dtu.dk, [3]vz@elektro.dtu.dk

***Abstract*—Magnetic Resonance Imaging (MRI) of nuclei other than 1H (e.g. 13C) allows for characterisation of metabolic processes. Imaging of such nuclei, however, requires development of sensitive MRI coils. This paper describes the design of surface receive coils for 13C imaging in small animals. The design is based on application-specified coil profile and includes impedance matching and balancing circuits. Active decoupling is implemented in order to minimize the influence of the receiving coil on the homogeneity of the transmit-coil field. Measurement results for a coil prototype are presented, including imaging experiments and estimation of the signal-to-noise ratio.**

I. Introduction

Imaging of 13C nuclei presents a wide variety of new applications including investigations of metabolism, biochemical analysis, elucidation of protein structures, and studies in polymer sciences [1]. In many of those applications, however, the level of the signal is low due to low 13C concentration as well as inherently low 13C signal strength. This requires an implementation of sensitive receiving coils. The work presented in this paper pertains to the design of receiving radio frequency (RF) coils for MRI imaging of 13C in small animals. RF coils are key components of MRI systems which determine the achievable signal-to-noise ratio, and consequently, the quality of the obtained MRI image.

MRI coils can roughly be divided into two categories, surface coils and volume coils. Volume coils image the entire sample. Surface coils can achieve a higher signal-to-noise ratio (SNR) by imaging only a portion of the sample. Only noise from that portion will be collected (disregarding electronic noise), and the signal will be higher due to the closer proximity of the portion to the coil, hence increasing SNR. Both coil types can be used alone for excitation and transmission. However, a surface coil generates an inhomogeneous field, and it is therefore better to use a volume coil to obtain a homogeneous excitation and a surface coil for the reception to obtain high SNR.

One challenge in RF coil design is matching the impedance of the RF coil. The input impedance of RF coils is highly inductive with a very low resistance (in the range of 1 Ω, or below), and it is not trivial to match the coil to standard 50 Ω of receiving circuitry.

Another challenge is that detuning occurs when the coil is placed in the vicinity of a sample. A fine-tuning of the impedance matching is necessary every time a new sample is imaged. One solution is to implement a tuning circuit external to the scanner bore.

When separate coils are used for transmission and reception of the RF signal, the interaction between the coils both disturbs the homogeneity of the RF transmit field and results in detuning of both coils. When both coils are impedance matched to the same frequency, they exhibit split-resonances when in close proximity of each other. To minimize this effect, a coil decoupling circuit has been developed. Externally controlled PIN diodes are actively open-circuited to introduce an LC filter. The RF current in the coil is blocked by the LC filter, even when the coil is exposed to a varying flux. This prevents the mutual coupling between two coils. Either coil must be 'turned off' when the other is operating (transmitting or receiving). Considering both passive and active decoupling methods, the latter is found more effective and is realized here.

The work presented in this article is based on the ideas in [2]. We present a systematic method to design surface coils for small animals: In II. A. we discuss choosing a coil geometry. In II. B. we discuss impedance matching circuit options. Then in II. C. a choice of active decoupling circuit topologies is presented.

II. Surface Coil Design

This section describes the design of a surface coil in three steps: A) Determining coil geometry from penetration depth requirements, B) determining a suitable matching network, C) choosing a suitable (passive or active) decoupling circuit topology.

A. Coil Geometry

Surface coil geometry is chosen according to the desired imaging depth where optimal SNR is desired. For a circular loop coil, the coil radius must approximately equal the penetration depth to obtain optimal SNR [3]. A larger radius results in excessive noise from outside the desired volume, and a smaller radius means lack of signal from the desired volume, both degrading the SNR. For imaging small animals, the circular loop radius will usually be in the order of a couple of centimeters.

B. Input Matching

The input impedance of a coil contains an inductive part and very low resistive part. The inductive part is due to the

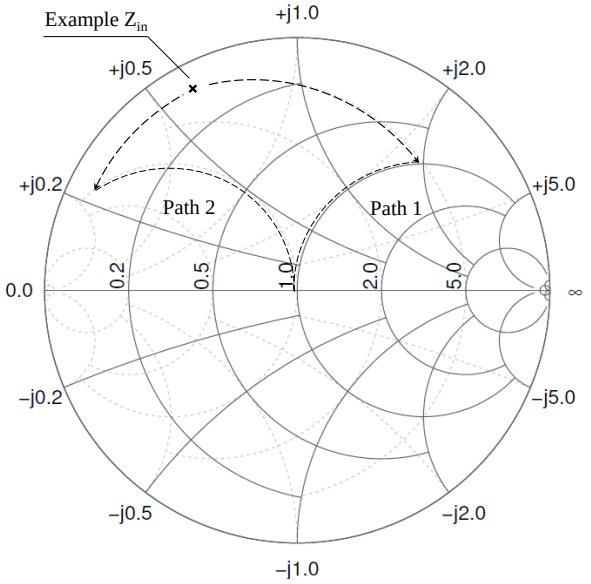

Figure 1. A Smith chart depicting two widely used matching networks for surface coils (resistive part of Z_{in} exaggerated for illustration purposes). Path 1 corresponds to the circuit in Fig. 2 (a), while Path 2 corresponds to the circuit in Fig. 2 (b). Both networks match the coil to 50 Ω, but the capacitor values vary drastically for the two networks used on the same coil.

geometry of the loop, and the resistance stems mainly from ohmic losses in the loop conductor and from electromagnetic coupling to the sample.

When a coil is connected to the RF receive circuitry with an impedance of 50 Ω it must be impedance matched to 50 Ω [2]. The impedance matching must be narrowband to increase SNR, meaning employing a single-stage high-Q matching network.

An example of a coil input impedance (with the resistive part greatly exaggerated for illustration purposes) is seen on Fig. 1. An impedance matching network, shown in Fig. 2 (a), employs a parallel capacitor that transforms the input impedance along the constant admittance line down to the 50 Ω line. A series capacitor removes the residual inductance by transforming the input impedance along the constant resistance line to the 50 Ω. This procedure is shown as Path 1 on Fig. 1.

An alternative impedance matching network, shown on Fig. 2 (b), is a reversed form of the previous. Here, the series capacitor is employed first, but inserted in the middle of the loop instead of at the loop terminals. The series capacitor cancels much of the inductance of the loop and transforms the input impedance along the constant resistance line to the 0.02 S line. Another parallel capacitor transforms the input impedance along the 0.02 S line to pure 50 Ω impedance. This procedure is shown as Path 2 on Fig. 1.

The network to choose depends on which of the realized capacitance values are practical, and whether the loop segmentation is desirable. Loop segmentation reduces the conservative $\bar{E}$-field in the sample, and this reduces loss. It also blocks DC current when using active decoupling. Segmentation might be

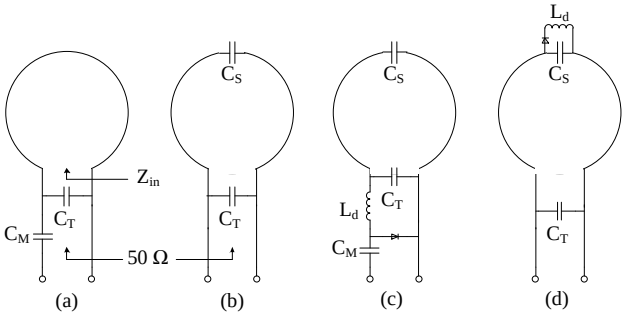

Figure 2. Matching networks for surface coils: (a) uses a tuning and matching capacitor, while (b) has the matching capacitor inserted in the loop and is then called a segmenting capacitor. (c) and (d) use a diode to introduce a parallel LC network to block any induced currents during an MR experiment. Depending on the application, it might be advantageous to have the loop segmented.

impractical if the loop size is too small, and one also has to ensure that the fringing fields from the capacitor does not enter the sample and incur more loss.

C. Active Decoupling

A surface coil must make use of a decoupling system when used in conjunction with a volume coil [2], [4]. The idea is to break the loop of the surface coil when the volume coil is transmitting. This is implemented using PIN diodes that are either reverse or forward biased. PIN diodes are not inserted directly into the loop for several reasons[1]. Instead, the diode introduces an LC filter that presents an infinite impedance at the desired frequency.

The networks on Fig. 2 (a) and (b) are seen augmented with an active decoupling network on Fig. 2 (c) and (d). When the diode is injected with sufficient DC current (forward biased), the resulting short-circuit makes inductor L_d resonate in parallel with a capacitor (C_T in (c), and C_S in (d)), causing the loop to be broken by the resulting (theoretically infinite) impedance. The actual impedance will be determined by the equivalent series resistance (ESR) or Q of the inductor and the ESR of the diode. A PIN diode must be chosen that has a sufficiently low resistance at the available biasing current (usually 20–100 mA), but for small surface coils it might be difficult to achieve the needed inductance value of L_d with a high enough Q.

Also note that for the circuit in Fig. 2 (c), RF chokes (not shown for simplicity) are employed to by-pass C_M when feeding the bias current through the feedline. Therefore, the loop also needs to be segmented by a capacitor C_S. The RF chokes are usually bulky and are a disadvantage of that particular implementation.

III. Circuit Realization

We implemented a coil using a symmetric variation of the circuit in Fig. 2 (c). The symmetry is to prevent strong

[1]The diode has high ohmic resistance compared to the loop which adds noise and reduces signal. The bias current is physically closer to the sample (as in Fig. 2 (d)), which can ruin the transmit field homogeneity.

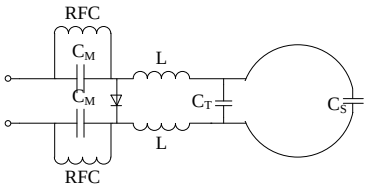

Figure 3. Schematic of the surface coil. C_T and C_M match the impedance to 50 Ω. The two inductors, L, resonate with C_T to decouple the coil when the diode is short-circuited. The RF chokes provide DC bias to the diode, and capacitor C_S acts as a DC block to prevent the loop from short-circuiting the diode.

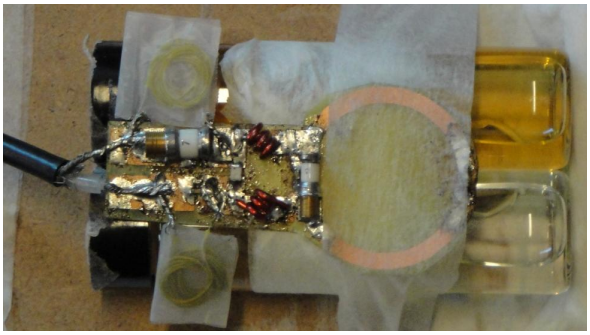

Figure 4. 13C surface coil, 3 cm in diameter, on top of two flasks with pyruvate and acetate. Two RF chokes (yellow) bypass the matching capacitors. The diode is seen between the two small solenoids, they resonate with the tunable capacitor to the right during diode short-circuit.

common-mode currents on the cable shield that detune the coil and results in reduced SNR [5]. The schematic for this coil is seen in Fig. 3. The coil consists of PCB traces on standard FR4, with a loop diameter of 3 cm and trace width of 3 mm, and is seen in Fig. 4.

A. Simulation and Matching

Ball-park values were estimated by modeling the coil structure in a full-wave electromagnetic simulator and then adjusted experimentally afterwards.

B. Active Decoupling

The active decoupling has been tested using a VNA by disconnecting the coil and connecting the VNA to the port that is seen by the coil (see Fig. 5). When the PIN-diode is reverse biased (open-circuited), the shunt capacitor C_T is seen by the VNA. When a biasing current is injected through the diode, its internal resistance drops exponentially with the increase in current, reaching about 1 Ω at full biasing. The resulting input impedance seen by the VNA is a parallel resonant network presenting an open-circuit at the resonance frequency. The more series resistance in the inductor and diode, the less perfect the short-circuit is. This is due to the approximation $R_p = (Q^2 + 1)R_s$ at the resonance frequency (where R_p is parallel resistance, and R_s is series resistance), because Q is low when R_s is high (see Fig. 6). On the Smith chart, when R_s increases, the resonance circle moves from the periphery of the chart inwards, which can be verified by decreasing the bias current through the diode (increasing R_s).

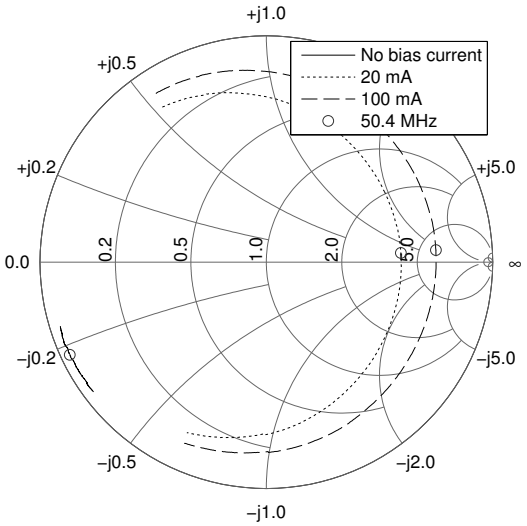

Figure 5. S-parameters of the LC network with different diode biasing currents. With no biasing current, mainly C_T is seen. When diode is short-circuited, C_T and L_d resonate, forming a Q-circle. The less resistance in the diode and inductor, the larger the Q-circle is, and the more perfect the open-circuit is (the small circle locates the 50.4 MHz frequency of 13C).

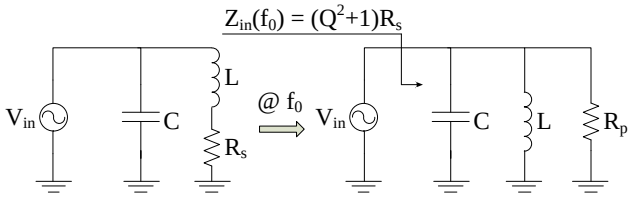

Figure 6. R_s models losses in inductor and diode. For ideal elements, $R_s = 0$, and the resulting impedance at resonance is infinite ($R_p \to \infty$). However, when R_s is increased, R_p is decreased.

C. Tuning Circuit

A external tuning circuit was made to provide additional tuning capabilities outside the scanner bore and to supply a path to the bias current through an RF choke.

The tuning box consists of an L-section matching network (see Fig. 7), where each branch can be either inductive or capacitive depending on the tuning of the capacitors. If the impedance of the coil is perfectly tuned to 50 Ω, the shunted branch (C_T,L_T) resonates in parallel causing an open-circuit, and the series branch (C_M,L_M) resonates causing a short-circuit, rendering the tuning box 'transparent' and the coil impedance is seen at the input of the tuning box. If the coil impedance is not exactly 50 Ω, it can be tuned by varying the capacitances. Since the coil is usually matched close to 50 Ω, the losses due to standing waves on the feedline between the tuning box and coil are reduced.

The inductance values are determined by assuming resonance when the capacitor is trimmed half-way, giving equal range to the inductive and capacitive side. Here, the variable capacitors (Voltronics NMNT15E) had a range of 1 pF–15 pF. Assuming a half-way trim of 7 pF, the resulting inductance value is $L = (\omega^2 C)^{-1} = 1.42$ μH (and assuming 13C

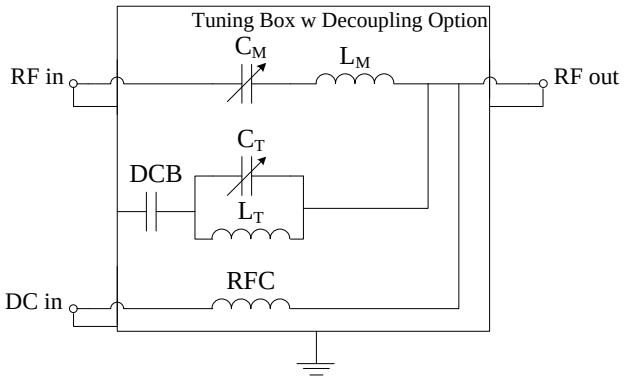

Figure 7. Schematic of tuning box with active decoupling option. The tunable capacitors (C_M,C_T) determines if the branches are inductive, capacitive, or zero impedance. The diode is short-circuited by a PIN diode driver connected to DC in through the RF choke, and the DC block capacitor prevents the driver from short-circuiting to ground.

resonance frequency $f_0 = 50.4$ MHz for a 4.7 T scanner).

The loop radius, R, and the number of windings, N, for the inductor can be determined using the classic inductance formula given in Eq. 1, where a is the wire radius, and μ_0, μ_r are the free-space and relative permeability of the wire, respectively. In our initial estimation, the inductors consist of copper wire of radius 0.5 mm, loop radius 1 cm, and six turns, which yields the inductance value 1.39 μH.

$$L_{loop} = N^2 R \mu_0 \mu_r \left(\ln\left(\frac{8R}{a}\right) - 2 \right) \quad (1)$$

We found that we needed around 4-5 turns likely due to parasitic elements. It is easy to fabricate the inductors with a slightly higher value than required, and then stretch the inductor to fine tune the inductance while verifying the resonance frequency with a VNA.

The RF choke is implemented using a simple wire-wound inductor presenting a high impedance to RF current. A ferrite core is not allowed due to the strong magnetic field of the scanner. There is no specific inductance to attain, but the reactance needs to be high enough, for instance $j1000\ \Omega$. The RF choke can be verified by using a VNA to determine the coil impedance. When the bias supply is connected through the RF choke, no change in input impedance should be observed with the VNA, otherwise the choke needs to be bigger. We used a tightly wound inductor with copper wire radius 0.5 mm, winding radius 1 cm, and 20 turns, having a length of about 3 cm.

IV. Results

We found the active decoupling to work well when the surface coil was used in conjunction with a volume coil. The experiment went as follows. The surface coil was placed on two vials with 13C-labelled acetate and pyruvate, both resonating around 50.4 MHz. Both the vials and surface coil were inserted into an 1H/13C volume transmit/receive coil from RAPID Biomedical GmbH and into the scanner bore (Varian, 4.7 T).

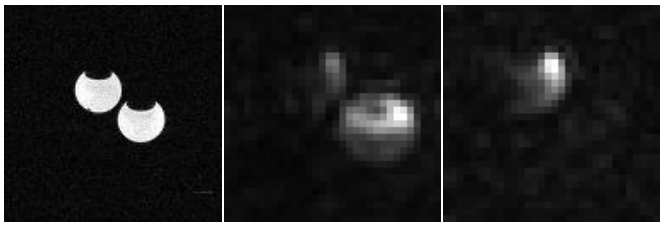

Figure 8. MRI image taken with the setup in Fig.4. The slice is transverse to the length of the flasks. Left: 1H image using commercially available volume coil. The black tops on each flask are air bubbles. Middle/Right: Pyruvate and Acetate respectively in the flasks resonating at slightly different frequencies around 50.4 MHz. Here, the volume coil is used to transmit and the surface coil is used to receive.

The result of the MR experiment in Fig. 4, taking the transverse slice of the two flasks, is seen on Fig. 8. The left image is taken with the volume coil in the 1H channel; the two others are taken with the surface coil in the 13C channel and using the volume coil in transmit-mode.

For that specific experiment, the SNR of our surface coil was 40 dB (or 100), which is comparable to 43 dB (or 140) obtained with an available surface coil (with a slightly smaller radius) in the same experiment.

V. Conclusions

A design method for surface receive coils has been shown. The design of the coil geometry was discussed, and various circuits implementing impedance matching and active decoupling have been shown. The design method has been verified experimentally, and a prototype of a coil was produced including matching and decoupling circuits as well as external tuning box. The circuits have been characterized and experimental results have been shown.

Acknowledgment

We would like to thank Lise Vejby Søgaard and Peter Magnusson from the Danish Research Centre for Magnetic Resonance (DRCMR) for acquisition and analysis of MR data.

References

[1] J. Ardenkjaer-Larsen, B. Fridlund, A. Gram, G. Hansson, L. Hansson, M. Lerche, R. Servin, M. Thaning, and K. Golman, "Increase in signal-to-noise ratio of $>$ 10,000 times in liquid-state NMR," *Proc Natl Acad Sci U S A.*, vol. 100(18):10, 2003.

[2] F. D. Doty, G. Entzminger, J. Kulkarni, K. Pamarthy, and J. P. Staab, "Review Article Radio frequency coil technology for small-animal MRI," *Simulation*, pp. 304–325, 2007.

[3] G. Giovannetti, F. Frijia, L. Menichetti, M. Milanesi, J. H. Ardenkjaer-Larsen, D. De Marchi, V. Hartwig, V. Positano, L. Landini, M. Lombardi, and M. F. Santarelli, "Hyperpolarized [sup 13]C MRS surface coil: Design and signal-to-noise ratio estimation," *Medical Physics*, vol. 37, no. 10, p. 5361, 2010.

[4] W. Edelstein, "Electronic decoupling of surface-coil receivers for NMR imaging and spectroscopy," *Journal of Magnetic Resonance (1969)*, vol. 67, no. 1, pp. 156–161, Mar. 1986.

[5] D. M. Peterson, B. L. Beck, G. R. Duensing, and J. R. Fitzsimmons, "Common mode signal rejection methods for MRI: Reduction of cable shield currents for high static magnetic field systems," *Concepts in Magnetic Resonance*, vol. 19B, no. 1, pp. 1–8, Oct. 2003.